Two-Dimensional Hard X-Ray Beam Compression by Combined Focusing and Waveguide Optics

A. Jarre,[1] C. Fuhse,[1] C. Ollinger,[1] J. Seeger,[1] R. Tucoulou,[2] and T. Salditt[1,*]

[1]*Institut für Röntgenphysik, Universität Göttingen, Geiststrasse 11, 37073 Göttingen, Germany*

[2]*European Synchrotron Radiation Facility (ESRF), 6 rue Jules Horowitz, 38043 Grenoble, France*

(Received 3 November 2004; published 24 February 2005)

A two-dimensionally confining x-ray channel waveguide structure is combined with a high gain Kirkpatrick-Baez prefocusing mirror system yielding a hard x-ray beam with a cross section of 25×47 nm^2 (FWHM). Unlike the previously employed resonant beam coupling scheme, the incoming beam is coupled in from the front side of the waveguide and the waveguided beam is no longer accompanied by spurious reflected or transmitted beams. The field distribution in the waveguide channel has been calculated numerically. The calculated transmission and far-field intensity pattern are in good agreement with the experimental results.

DOI: 10.1103/PhysRevLett.94.074801 PACS numbers: 41.50.+h, 42.82.Et, 61.10.–i

An efficient focusing or compression of hard x rays to the smallest possible beam sizes can lead to novel applications in diffraction, spectroscopy, and imaging. ''Classical'' x-ray experiments probe molecular structures far in the thermodynamic limit of large system size, since typically beam cross sections are many orders of magnitude larger than the wavelength λ. Recent progress in reflective, refractive, and diffractive optical elements has pushed the limits of small and intense x-ray beams to the micron and submicron range. Well-known examples include adaptive Kirkpatrick-Baez (KB) mirrors [1], compound refractive lenses [2], capillary optics [3], as well as hard x-ray Fresnel zone plates [4] and Bragg-Fresnel lenses [5]. At the same time Bergemann, Keymeulen, and van der Veen have raised the fundamental question of the smallest possible focus size and have argued that it is determined by the x-ray index of refraction $n = 1 - \delta + i\beta$ rather than by the Abbé limit [6]. According to their arguments, the limit is identical to the smallest dimension $\sim W_C$ of a waveguided x-ray beam, depending only on the internal critical angle Θ_C determined by the electron density of the waveguide cladding

$$W_C = \frac{1}{2}\frac{\lambda}{\Theta_C} = \frac{1}{2}\frac{\lambda}{\sqrt{2\delta}} = \frac{1}{2}\sqrt{\frac{\pi}{r_e n_e}}, \qquad (1)$$

with the classical electron radius r_e and the electron density n_e of the cladding material. For planar x-ray waveguides (XWG), mode propagation has been observed for guiding layer thicknesses down to $d \simeq 10$ nm [7], almost reaching this limit.

Apart from the small beam sizes, several other properties make x-ray waveguides attractive: (i) the internal field distribution in phase and amplitude is exactly given by the solution of the Helmholtz equation, (ii) the tails of the beam are decaying exponentially, and (iii) XWGs act as spatial as well as coherence filters for the incoming radiation, at least in the case of monomodal resonators.

Different schemes of coupling the x-ray beam into the (planar) waveguide have been probed, e.g., the resonant beam coupling (RBC) scheme where an evanescent wave is coupled into the guiding layer through a thin cladding [8–11]. Another coupling technique makes use of a standing wave field in front of the device [12]. In the front-coupling scheme used here, the beam is coupled in directly from the front side, as recently demonstrated for a planar monomodal waveguide [13]. Recently, two-dimensional (2D) waveguide structures fabricated by *e*-beam lithography have been tested in the RBC scheme [14]. However, the total flux in such devices is too poor for most applications. In the proof-of-principle experiment, resonant x-ray modes have been observed, with a 70-fold gain in flux density. Furthermore, the waveguide beam was accompanied by spurious specular reflected and transmitted beams originating from the RBC coupling scheme. These can be eliminated by making use of front-coupling waveguides (FCWs) where unwanted radiation is absorbed in the cladding [13]. However, for FCWs the total count rate would be even lower than for RBC-XWGs in a comparable setup, since they do not provide an intrinsic increase in flux density. Yet, another property of FCWs can be exploited to increase the total flux of the waveguided beam tremendously: The angular acceptance of FCWs lies in the range of some hundredths of a degree (while it is in the range of a few thousandths of a degree for RBC-XWGs). This high value matches the focusing angle of the presently most efficient focusing x-ray optics. The combination of such optics to increase the total flux, and a 2D x-ray waveguide to set the beam dimensions and properties, can thus provide well defined, intense hard x-ray nanobeams. In this Letter, we present a combination of a high gain adaptive KB mirror and a 2D XWG exhibiting an overall gain in flux density of $g \simeq 4000$ (flux density before KB optics over flux density behind the 2D XWG) and providing a beam size of 25×47 nm^2 [full width at half maximum (FWHM)], which is the smallest beam size published so far for hard x rays. We

furthermore show that the exiting beam properties can be obtained from numerical simulations.

The electric field u in the waveguide can be calculated starting from the Helmholtz equation

$$\Delta u + n^2 k_0^2 u = 0 \tag{2}$$

with the Laplace operator Δ and $k_0 = 2\pi/\lambda$. In order to find the optimum XWG design and, in the future, to determine the field distribution for imaging applications, we have calculated the electric field inside the guide by means of a finite-difference approach solving Eq. (2) in the approximation of the parabolic wave equation [15]. The parabolic wave equation is obtained from the Helmholtz equation using the ansatz $u(x, y, z) = \psi(x, y, z)e^{-ik_0 x}$ and neglecting the second derivative $\frac{\partial^2}{\partial x^2}\psi(x, y, z)$, leading to

$$\left(\frac{\partial^2}{\partial y^2} + \frac{\partial^2}{\partial z^2} - 2ik_0\frac{\partial}{\partial x}\right)\psi + [k_0^2(n_j^2 - 1)]\psi = 0, \tag{3}$$

with the index j denoting the respective materials (core and cladding). A simulation of the electric field inside the experimentally characterized 2D XWG with core dimensions of 30×70 nm^2 [Fig. 1(b)] is presented in Fig. 2; the respective integrated far-field intensity distribution is shown in Fig.4. The far field $\mathcal{I}(\varphi_f, \Theta_f)$ is obtained from the electric field $\Psi(y, z)$ at the exit of the guide via the relation

$$\mathcal{I}(\varphi_f, \Theta_f) = \mathcal{I}_0 \left| \int_{-\infty}^{+\infty} \Psi(y, z)e^{ik_0(\varphi_f y + \Theta_f z)}dydz \right|^2, \tag{4}$$

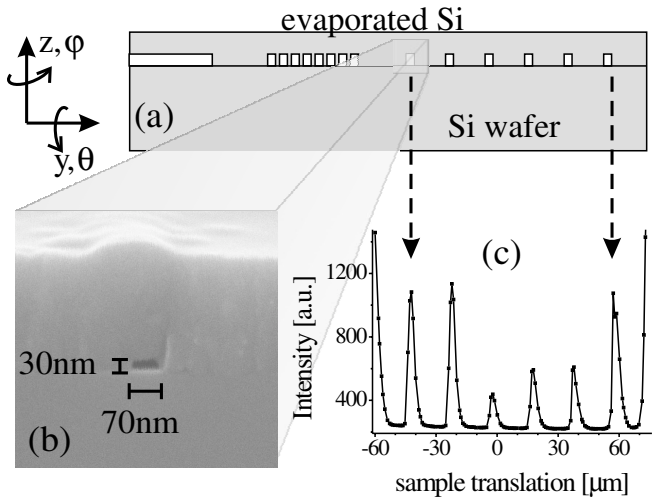

FIG. 1. (a) The lithographic structure consisting of planar waveguides (left), a grating (middle), and several separated 2D waveguides. (c) The angularly aligned structure is translated through the focus of the Kirkpatrick-Baez mirror system to locate the positions of the individual waveguide channels. (b) Scanning electron microscopy micrograph showing the front side of a 2D XWG.

where the far-field angles are taken with respect to the normal of the exit plane of the waveguide.

The 2D XWGs were prepared by spin coating a $d_1 = 44$ nm layer of the polymer polymethyl methacrylate (PMMA) on a Si (100) wafer (Silchem) [16]. This polymer layer was used as a positive resist for electron beam lithography (Lion LVI, Leica). During the lithography process, narrow lines ($d_2 = 60$–100 nm) were left unexposed in between comparatively large areas (width = 20 μm; length = 10 mm) of complete e-beam exposure. The unexposed strips of the polymer remaining on the Si substrate after development of the PMMA film were later used as the low density waveguide core material. During the developing process [in a 4:1 mixture of ethylene glycol monoethyl ether ($C_4H_{10}O_2$) and ethylene glycol monobutyl ether ($C_6H_{14}O_2$)] the height of the unexposed stripes was reduced to 30 nm. A 300 nm thick layer of Si was evaporated (UNIVEX 450, Leybold) on top of the developed wafer, generating a symmetric Si cladding around the PMMA core (guiding channel); see Fig. 1. In a final step, the device was cut to the desired length $l = 4.05$ mm corresponding to a transmission through silicon of $T_{\mathrm{Si}} = 1.5 \times 10^{-7}$ at an x-ray energy of $E = 12.5$ keV. Note that high aspect ratios (length/width) of $>10^4$ are achieved by this technique. They are needed to block the primary beam in the cladding, i.e., in the overilluminated parts of the 2D XWG front side around the PMMA core. In order to facilitate the alignment of the 2D XWGs, broad areas of the PMMA were kept unexposed during the lithography process. After development and evaporation, these areas act as planar waveguides [13], which were used to align the vertical incidence angle Θ_i. In addition,

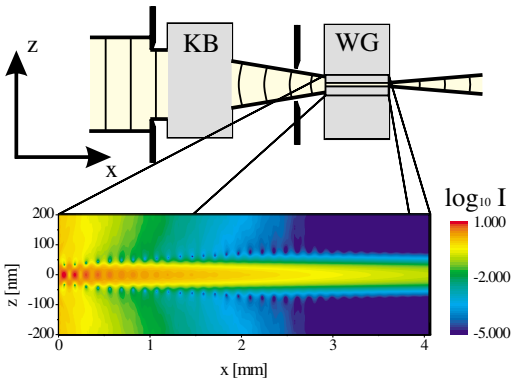

FIG. 2 (color). Schematic of the experimental setup: the 2D-XWG structure is aligned in the focus of a Kirkpatrick-Baez mirror system. The focused beam is coupled into the front side of the waveguide and propagates in the WG core, as illustrated by the numerical simulation of the device: The intensity of the electric field in the 2D XWG is shown in logarithmic color scales. The overilluminating parts of the beam are damped in the absorbing cladding. Only the waveguided beam, without side peaks, spurious reflected, or primary beams, is extracted at the exit of the structure.

a grating of 100 lines (repeat distance 300 nm, aspect ratio 1:1) was written in the resist providing a grating of 2D waveguides and facilitating the alignment of the horizontal incidence angle φ_i. To block the primary beam passing above the evaporated top cladding layer, an additional stripe of lead (height $\sim$2 mm) was glued atop the guide with silver lacquer. The experiment was carried out at the ID22 undulator beam line at the European Synchrotron Radiation Facility in Grenoble, France. The x-ray energy was set to 12.5 keV by a Si (111) double monochromator. Higher harmonics of the undulator were suppressed by (i) detuning of the monochromators, (ii) a Si mirror tilted to 0.14°, and (iii) the adaptive KB optics [17,18]. An aperture of 1×1 mm^2 defined the incident beam in front of the prefocusing KB mirrors. The KB system provided a focal spot size of 2.5×3.8 μm^2 (vertically $\times$ horizontally), as measured by knife edge fluorescence (Au L-edge) scans. In order to reduce the background an additional $d_{\mathrm{pin}} = 20$ μm pinhole was mounted behind the KB optics. Four detectors were used during the experiment: a fast scintillation detector (Cyberstar, Oxford instruments) placed 470 mm behind the focus, a CCD system (TE/CCD-1242-EM/1, Princeton Instruments, pixel size 22.5×22.5 μm with optical magnification of the image taken on a scintillation foil) placed 170 mm behind the focus, as well as a semiconductor fluorescence detector and a diode to measure the integrated flux at all positions of the setup. All count rates given in this Letter are scaled to a ring current of 180 mA. A schematic of the experimental setup is shown in Fig. 2. The intensity of the primary beam was measured to 7.7×10^{11} photons/s/mm^2. The KB focusing optics provided 3.3×10^{11} photons/s in a spot size of 2.5×3.8 μm^2. The entrance of the 2D waveguide [30×70 nm^2 (vertical $\times$ horizontal)] was thus overilluminated by a factor of $\sim 4.5 \times 10^3$, i.e., 7.3×10^7 photons/s (0.02% of the focused beam) hit the waveguide entrance. Behind the device, 3.5×10^6 photons/s were detected, corresponding to an efficiency of the waveguide of 4.7% (number of photons hitting the waveguide entrance over the number of photons exiting the device), while the simulations predict an efficiency of 5.6% for an incoming plane wave. Taking into account the angular acceptance of the waveguide, which can be estimated to $\simeq 80\%$ from the angular distribution of the far field, the agreement between experimentally obtained count rates and the simulated intensity is within 5%. The entirely different optical properties of the beams produced by (i) only the KB system and (ii) the filtered beam produced by the combined optics is illustrated by the CCD images obtained in the far field; see Fig. 3. While the KB image shows small scale interference fringes, such a fine structure is not observed in the waveguided beam. In the latter case the profile is particularly clean along the vertical axis reflecting the monomodal behavior achieved due to the small waveguide height, while the horizontal profile shows some intensity variation indicative of multimodal excitation. The respective far-field profiles were investigated in more detail by orthogonal line scans using scintillation counters. The measured scans through the far field both in the vertical and the horizontal direction are shown in Fig. 4 (symbols). The lines in the graph represent an integration of the simulated far field in one direction (corresponding to the perpendicular scan direction). The simulations were scaled to the measured intensity, while the scaling factor is the same for both directions. Since the calculations were performed with a grid spacing of 1 nm both in the vertical and the horizontal direction, the ''field of view'' during the calculation was reduced to 800×800 nm^2 in order to reduce computing time. Because of this, the background is too low in the simulations compared to the measurements. The measured background was therefore added to the simulation. The calculation is in very good agreement with the measured data concerning the vertical scan direction, while small deviations are observed between the simulation and the tails of the horizontal far-field distribution. The vertical side length of the rectangular WG was 30 nm. This implies guiding of a single mode only [19]. Therefore, small variations of the incidence angle Θ_i do not affect the *shape* of the far field in this direction. In contrast, the horizontal dimension of the guide was 70 nm; i.e., the guide exhibits multimodal behavior. Because of mode mixing in the guide, the shape of the far field is highly sensitive to the incidence angle φ_i, which explains the observation.

In conclusion, the combination of a high gain KB mirror system and a 2D-XWG nanostructure fabricated by e-beam lithography has been used to produce a 12.5 keV beam with a cross section of 25×47 nm^2 (FWHM), as evidenced from the far-field distribution of the exiting beam. A flux density enhancement (gain) of $g \sim 4000$ was observed for the combined KB-2D-XWG system. We point out that owing to the filtering properties of the waveguide, this beam is not accompanied by disturbing side peaks or spurious reflected and primary beams, which present a source of complication in imaging or diffraction

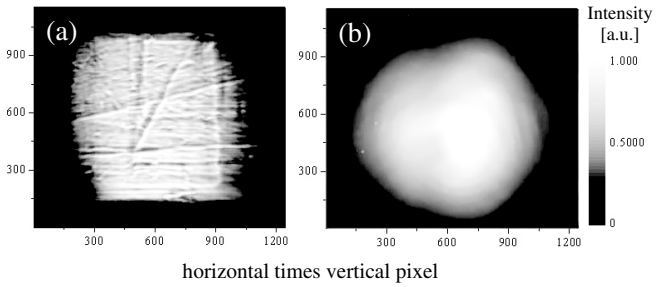

FIG. 3. CCD images of the beam defined (a) by only the Kirkpatrick-Baez focusing optics and (b) by the combined focusing and waveguiding optics, both taken 170 mm behind the focal spot of the KB optics illustrating the filtering properties of the 2D waveguide structure.

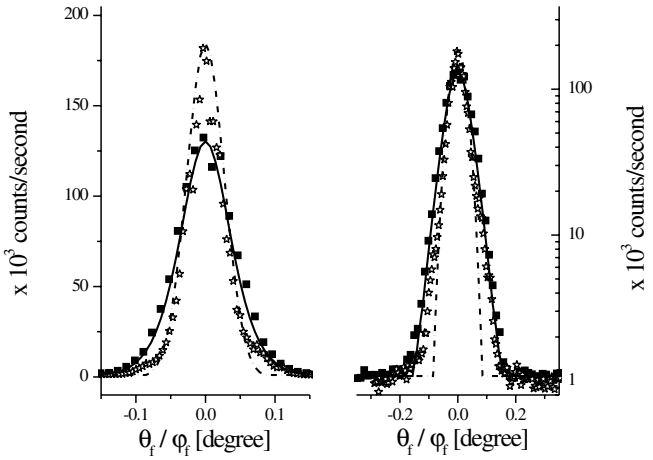

FIG. 4. Measured far-field pattern of the waveguided beam in the vertical (solid squares) and the horizontal (open stars) direction, both in linear (left) and logarithmic (right) scales. The lines show the simulated far field of a 2D XWG with a PMMA guiding layer of 30×70 nm^2 (solid line: vertical; dashed line: horizontal). These values correspond to a beam size of 25×47 nm^2 (FWHM) in the near field and directly behind the 2D-XWG structure.

applications. The field distribution corresponds to an eigenstate or superposition of eigenstates (modes) of the waveguide structure and is therefore quantitatively predictable. This is an important requirement for projection phase microscopy (inline Gabor holography), using the quasi point source of an x-ray waveguide for sample illumination. Illumination of nm-sized samples by a coherent WG beam and the observation of the far-field intensity pattern will allow for the reconstruction of the electron density of the sample. Holographic reconstruction may also be combined with oversampling algorithms which are presently investigated for hard x rays [21]. The present scheme can be further improved by using higher demagnification ratios of the KB optics and hence smaller overillumination, in combination with a 2D XWG of down to a 10 nm cross section and improved efficiency. A 2D XWG of this size is necessarily monomodal in both directions, leading to a spatially coherent exit beam and would reach the predicted fundamental limit [6]. Furthermore, the ideal 2D XWG might consist of a vacuum instead of a polymer core and could be fabricated by other techniques than shown here, such as wafer bonding, focused ion beams, or by templating from stiff biopolymers or nanotubes.

We acknowledge Silvain Bohic of the ID22 beam line for help during the experiment, the European Synchrotron Radiation Facility for provision of synchrotron radiation facilities, and the Ministry of Research BMBF for funding through Project No. 05KS4MGA/9. We thank Thorsten Gronemann and Jochen Herbst for technical assistance in WG fabrication.

*Electronic address: tsaldit@gwdg.de

[1] K. Yamauchi, K. Yamamura, H. Mimura, Y. Sano, A. Saito, A. Souvorov, M. Yabashi, K. Tamasaku, T. Ishikawa, and Y. Mori, J. Synchrotron Radiat. **9**, 313 (2002).
[2] C. G. Schroer *et al.*, Appl. Phys. Lett. **82**, 1485 (2003).
[3] D. H. Bilderback and D. J. Thiel, Rev. Sci. Instrum. **66**, 2059 (1995).
[4] C. David, B. Nöhammer, and E. Ziegler, Appl. Phys. Lett. **79**, 1088 (2001).
[5] Y. Li, M. Yasa, O. Pelletier, C. R. Safinya, E. Caine, E. E. Hu and P. Fernandez, Appl. Phys. Lett. **82**, 2538 (2003).
[6] C. Bergemann, H. Keymeulen, and J. F. van der Veen, Phys. Rev. Lett. **91**, 204801 (2003).
[7] F. Pfeiffer, T. Salditt, P. Hoghoj, I. Anderson, and N. Schell, Phys. Rev. B **62**, 16 939 (2000).
[8] Y. P. Feng, S. K. Sinha, H. W. Deckman, J. B. Hastings, and D. P. Siddons, Phys. Rev. Lett. **71**, 537 (1993).
[9] S. Lagomarsino, A. Cedola, P. Cloetens, S. DiFonzo, W. Jark, G. Souillé, and C. Riekel, Appl. Phys. Lett. **71**, 2557 (1997).
[10] S. Di Fonzo, W. Jark, S. Lagomarsino, C. Giannini, L. De Caro, A. Cedola, and M. Müller, Nature (London) **403**, 638 (2000).
[11] A. Jarre and T. Salditt and T. Panzner, and U. Pietsch, Appl. Phys. Lett. **85**, 161 (2004).
[12] M. J. Zwanenburg, J. F. Peters, J. H. H. Bongaerts, S. A. de Vries, D. L. Abernathy, and J. F. van der Veen, Phys. Rev. Lett. **82**, 1696 (1999).
[13] C. Fuhse, A. Jarre, C. Ollinger, J. Seeger, and T. Salditt, Appl. Phys. Lett. **85**, 1907 (2004).
[14] F. Pfeiffer, C. David, M. Burghammer, and T. Salditt, Science **297**, 230 (2002).
[15] Y. V. Kopylov, A. V. Popov, and A. V. Vinogradov, Opt. Commun. **118**, 619 (1995).
[16] 18 μl of a solution of the polymer in (2-methoxethyl) acetate at a polymer concentration of 2 mg/ml were spin coated at $\omega = 7000$ rpm. The thickness of the PMMA layer was analyzed by x-ray reflectivity measurements.
[17] O. Hignette, P. Cloetens, W.-K. Lee, W. Ludwig, and G. Roasting, J. Phys. IV (France) **104**, 231 (2003).
[18] Y. Dabin, G. Rostaing, O. Hignette, A. Rommeveaux, and A. K. Freund, Proc. SPIE Int. Soc. Opt. Eng. **4782**, 235 (2002)
[19] There is only one solution to the transcendental eigenvalue equation. See also [20].
[20] D. Marcuse, *Theory of Dielectric Optical Waveguides* (Academic Press, New York, 1974).
[21] J. Miao, T. Ishikawa, B. Johnson, E. H. Anderson, B. Lai, and K. O. Hodgson, Phys. Rev. Lett. **89**, 088303 (2002).